DIVERSE ALTERATION OF DOM 08006 (CO3.0) AND DOM 08004 (CO3.1) AND ITS EFFECT ON OXYGEN ISOTOPIC COMPOSITIONS OF GROSSITE-BEARING REFRACTORY INCLUSIONS. A. N. Krot[1*], K. Nagashima[1], and S. B. Simon[2] [1]HIGP/SOEST, University of Hawai'i at Mānoa, Honolulu, HI 96821, USA (*sasha@higp.hawaii.edu); [2]Dept. of the Geophysical Sciences, The University of Chicago, Chicago, IL 60637, USA.

Introduction: Most Ca,Al-rich inclusions (CAIs) in chondrites of petrologic type ≤ 3.0 (CO, CR, CM) are uniformly ^{16}O-rich ($\Delta^{17}O \sim -24‰$) suggesting formation in a gas of approximately solar composition [1, 2]. In contrast, melilite and anorthite in CAIs from CO and CV chondrites of higher petrologic type (≥3.1) are often ^{16}O-depleted to various degrees [3,4], indicative of postcrystallization exchange with an ^{16}O-poor external reservoir. The place and mechanism of this exchange (gas-melt or gas-solid in the nebula *vs.* fluid-rock on the parent bodies) remain controversial [4–6]. In our companion abstract [7], we reported on the mineralogy, petrography and O-isotope compositions (only in DOM 08004) of grossite-bearing CAIs in DOM 08004, *6* (CO3.1) and DOM 08006, *56* (CO3.00) (classification is based on Cr_2O_3 contents in chondrule ferroan olivines [8–10, this study]). In DOM 08004, grossite-bearing CAIs are isotopically heterogeneous with grossite ($\Delta^{17}O = -11‰$ to 0‰), and, in most cases, melilite ($\Delta^{17}O = -15‰$ to –1‰) being ^{16}O-depleted relative to hibonite, spinel, and Al,Ti-diopside ($\Delta^{17}O \sim -24‰$). In DOM 08004, grossite experienced incipient replacement by Fe-rich phases(s); in DOM 08006, it is petrographically pristine. Both meteorites experienced asteroidal alteration resulting in formation of phyllosilicates and abundant magnetite [9–12]. To understand possible effect of this alteration on the O-isotope compositions of grossite-bearing CAIs, we studied secondary mineralization of DOM 08004 and 08006 by the UH field emission electron microprobe JEOL JXA-8500F. Oxygen-isotope compositions of magnetite to be measured *in situ* with the UH Cameca ims-1280 will be reported at the meeting.

Secondary mineralization in DOM 08004 (CO3.1): Most Fe,Ni-metal nodules in chondrules are pseudomorphically replaced by Cr-bearing magnetite and Ni-rich metal, and often overgrown by clean Cr-free magnetite (Fig. 1a). Chondrule mesostasis is partially replaced by phyllosilicates. The most extensive alterationwas is found in silica-bearing pyroxene chondrules, in which silica is nearly completely pseudomorphically replaced by Fe-rich hydrous phase(s) (in wt%, 26.5 SiO_2, 0.93 Al_2O_3, 61.5 FeO, 0.62 MnO, 4.6 MgO, 0.2 CaO, 0.14 Na_2O, Σ = 94.5; "sec" in Fig. 1b). Some olivines in type I and type II chondrule fragments are overgrown by nearly pure fayalite (Figs. 1c,d). Matrix and fine-grained chondrule rims contain abundant submicron-sized grains of ferroan olivine, and are occasionally crosscut by fayalite veins (Fig. 1b). In addition, the matrix contains abundant coarse euhedral-to-subhedral magnetite grains associated with Ni-rich metal and

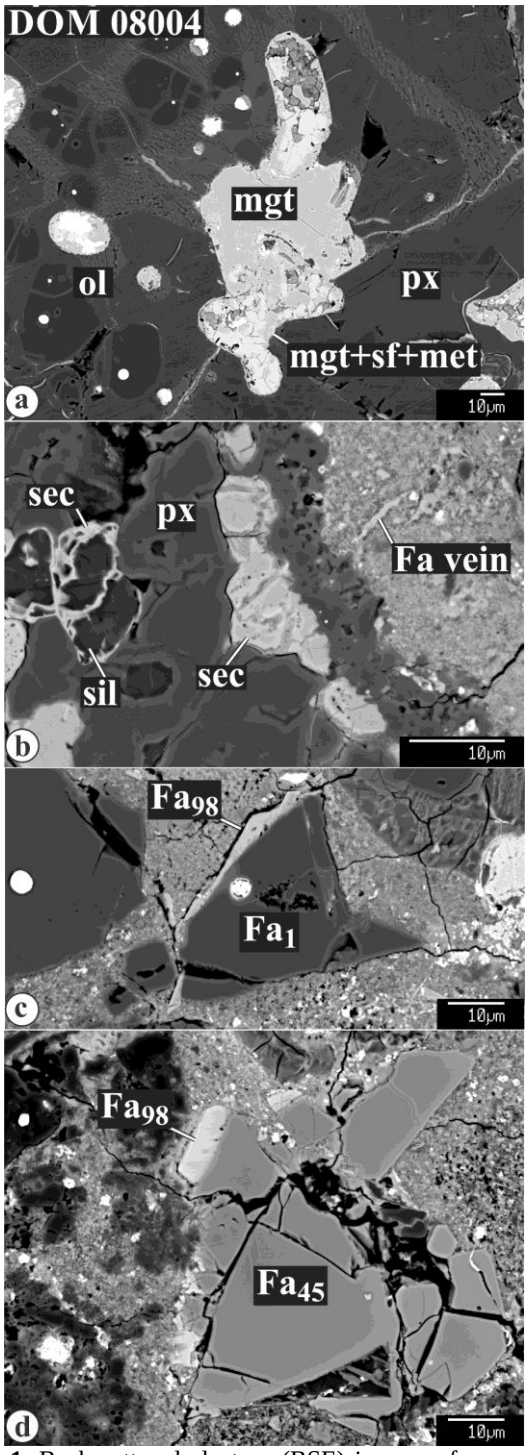

Fig. 1. Backscattered electron (BSE) images of secondary mineralization in DOM 08004 (CO3.1). met = Fe,Ni-metal; mgt = magnetite; ol = olivine; phyl = phyllosilicates; px = low-Ca pyroxene; sec = secondary Fe-rich hydrous phase(s); sf = sulfide; sil = silica.

troilite; Fe,Ni-carbides are exceptionally rare. Texturally and mineralogically similar secondary mineral assemblages have been described in MAC 88107 (CO3.1-like) and Kaba (CV3.1) [6,13]. DOM 08004 is brecciated and contains fragments of nearly completely hydrated chondritic clasts.

Secondary mineralization in DOM 08006 (CO3.00): Alteration of opaque nodules and mesostasis in chondrules is similar to that in DOM 08004. Matrix and fine-grained chondrule rims, however, contain abundant Fe,Ni-carbides (Figs. 2a–c), and, occasionally, crosscut by Fe,Ni-carbide veins (Fig. 2d); no secondary fayalite was found. In addition, the matrix contains abundant rounded magnetite nodules and coarse euhedral-to-subhedral magnetite grains associated with Ni-rich metal, troilite, pentlandite, and Fe,Ni-carbides. Texturally and mineralogically similar carbide-magnetite-bearing assemblages have been described in Semarkona (LL3.0) [14] and ALHA 77307 (CO3.0) [15]. DOM 08006 is brecciated and contains fragments of thermally metamorphosed chondritic material.

Discussion: Based on our mineralogical observations of DOM 08004, and thermodynamic analysis and isotopic data reported for fayalite-magnetite asseblages in Kaba and MAC 88107 [6, 13, 16], we infer that DOM 08004 experienced relatively high-temperaure (~100–300°C) hydrothermal alteration at a low water/rock ratio (<0.2). Krot and Nagashima [6] showed that anorthite and melilite in Kaba CAIs experienced O-isotope exchange with an asteroidal fluid responsible for the formation of fayalite and magnetite in that meteorite. We suggest that the ^{16}O-depleted compositions of grossite and melilite in the DOM 08004 CAIs [7] could have resulted from postcrystallization isotope exchange during fluid-rock interaction on the CO chondrite parent body. Δ^{17}O value of the fluid will be constrained by O-isotope compositions of fayalite and magnetite in DOM 08004, to be measured. DOM 08006 appears to have experienced relatively low temperature, Semarkona-like alteration, resulting in formation of carbide-magnetite assemblages. Therefore, it is expected that grossite-bearing CAIs in DOM 08006 have retained their initial O-isotope compositions. SIMS measurements of these CAIs are in progress and will be reported at the meeting.

References: [1] Makide K. et al. (2013) *GCA*, *73*, 5018–5051. [2] Kööp L. et al. (2016) *GCA*, *184*, 151–172. [3] Itoh et al. (2004) *GCA*, *68*, 183–194. [4] Simon J. et al. (2011) *Science*, *331*, 1175–1777. [5] Yurimoto H. et al. (2008) *Rev. Min. Geochem.*, *68*, 141–187. [6] Krot A. & Nagashima K. (2016) *MAPS*, *51(Suppl.)*, #1604. [7] Simon S. et al. (2017) *LPS*, *48*, this vol. [8] Grossman J. & Brearley A. (2005) *MAPS*, *40*, 80–122. [9] Davidson J. et al. (2014) *LPS*, *45*, #1384. [10] Simon S. & Grossman L. (2015) MAPS, 50, 1032–1049. [11] Howard K. et al. (2014) *LPS*, *45*, #1830. [12] Alexander C.M.O'D. et al. (2014) *LPS*, *45*, #2667. [13] Doyle P. et al. (2015) *Nature Commm.*, *6*, 1–10. [14] Krot A. et al. (1997) *GCA*, *61*, 219–237. [15] Scott E. & Jones R. (1990) *GCA*, *54*, 2485–2502. [16] Zolotov M. et al. (2006) *MAPS*, *41*, 1775–1796.

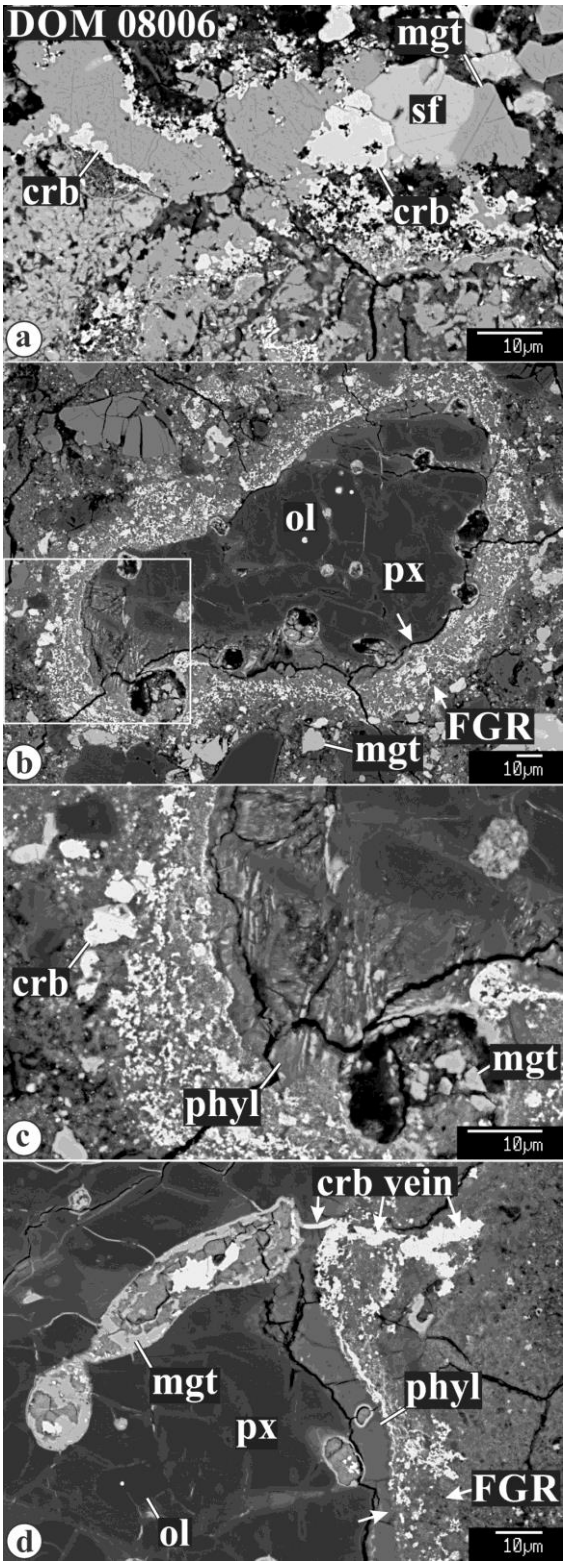

Fig. 2. BSE images of secondary mineralization in DOM 08006 (CO3.0). Region outlined in "b" is shown in detail in "c". crb = Fe,Ni-carbides; FGR = fine-grained rim; mgt = magnetite; ol = olivine; phyl = phyllosilicates; px = low-Ca pyroxene; sf = sulfide.